Electronic Journal of Biotechnology 34 (2018) 1–8

Contents lists available at ScienceDirect

Electronic Journal of Biotechnology

Research article

Kinetic modeling of the simultaneous production of ethanol and fructose by *Saccharomyces cerevisiae*

Ashraf K. Sulieman [a], Meilana Dharma Putra [b,*], Ahmed E. Abasaeed [a], Mohamed H. Gaily [a], Saeed M. Al-Zahrani [a], Mohamed A. Zeinelabdeen [a]

[a] *Department of Chemical Engineering, College of Engineering, King Saud University, P.O. Box 800, Riyadh 11421, Saudi Arabia*
[b] *Chemical Engineering Department, Faculty of Engineering, Lambung Mangkurat University, Banjarmasin 70123, Indonesia*

ARTICLE INFO

Article history:
Received 1 February 2018
Accepted 20 April 2018
Available online 30 April 2018

Keywords:
Bioreactor
Biosynthesis of ethanol
Ethanol
Fermenters
Fructose
Kinetic modeling
Kinetic models for ethanol biosynthesis
Kinetic models for fructose biosynthesis
Microbiological biosynthesis
Saccharomyces cerevisiae
Yeast

ABSTRACT

Background: Ethanol and fructose are two important industrial products that enjoy many uses. In this contribution, their production via selective fermentation of date extract using *Saccharomyces cerevisiae* was studied. Scaling up the process for possible commercialization was investigated in three fermentors with working volume ratio of 1:40:400.

Results: Higher ethanol concentration was obtained in the larger fermentor due to conversion of fructose. Fructose yields in the 0.5-L, 7.5-L and 80-L fermentors were 99, 92 and 90%, respectively. Good fitting was obtained with the modified Monod kinetics; however, a better fit of cell mass was obtained with the modified Ghose–Tyagi model which accounts for ethanol inhibition.

Conclusions: The modified Gompertz model was expanded to facilitate prediction of products' formation and fructose fractions in all three fermentors. Such expansion will be beneficial in industrial applications.

How to cite: Sulieman AK, Putra MD, Abasaeed AE, et al. Kinetic modeling of the simultaneous production of ethanol and fructose by *Saccharomyces cerevisiae*. Electron J Biotechnol 2018;34. https://doi.org/10.1016/j.ejbt.2018.04.006.

1. Introduction

Ethanol is one of the most potential products used in various applications. It is used as a solvent, a fuel, a chemical reagent, and a raw material for many important chemicals [1]. In North and South America, bioethanol was primarily sourced from starch, sugars and molasses [2]; on the other hand, USA and Brazil are the largest ethanol producer [3]. However, the demand for ethanol is steadily increasing especially as an energy source [4,5]. It is because the annual worldwide production of oil fuel is projected to reduce from 25 billion barrels in 2002 to about 5 billion barrels in 2050 [6]. Compared to fuel of gasoline, ethanol is renewable, non-toxic, easy to handle, safe to store, and sulfur-free; thus less contribution to global warming and air pollution [7,8].

Fructose, the sweetest natural sugar, is commercially used for foods, confectionery and beverages industries [9]. The fructose is 1.73 times sweeter than sucrose and about twice the sweetness of glucose; thus lesser amounts (subsequently calories) are needed. Fructose is recommended to use rather than other sweeteners because it is difficult to crystallize from an aqueous solution, faster to absorb moisture and slower to release it to the environment [10,11].

Over 8 million tons of date fruits have been produced in 2010 worldwide [12]. Unfortunately, almost half production of date is still unutilized [13]. About half of the date content is fructose; thereby providing a large opportunity for its production. Hydrolysis of starch followed by enzymatic isomerization process has been widely used in industry to convert glucose to fructose; unfortunately only about 42% HFS (high fructose syrup) was obtained due to equilibrium limitations [14,15]. On the other hand, 90% HFS can be produced via multistage chromatographic process [16], membrane technology [17], and ionic liquids [18]; such methods suffer from high production cost [19]. The development of various methods are still continuously researched such as the usage of nanofiltration [20], microalgae [21], and beverage waste [22] and inulin [23,24]. A very promising technique (still in its infancy) for the production of fructose from sugar mixtures is selective fermentation of glucose and other sugars (except fructose) to bioethanol [25].

Compared to other microbes, the utilization of *Saccharomyces cerevisiae* has been shown to suppress the high consumption of fructose and the formation of by-products such as sorbitol [26]. The

* Corresponding author.
E-mail address: mdputra@unlam.ac.id (M.D. Putra).
Peer review under responsibility of Pontificia Universidad Católica de Valparaíso.

https://doi.org/10.1016/j.ejbt.2018.04.006

performance of *S. cerevisiae* ATCC 36858 in media composed of sucrose, beet molasses and date syrup has been utilized [25,27]. Therefore, it is imperative to study the scale up of selective fermentation before launching an industrial production [28]. Kinetic models are valuable tools in understanding the behavior of the fermentation process that paves the way for further process development or industrial application. The classical Monod equation [29] has been proposed to elucidate the yeast performance during fermentation. However, it is interesting to study a kinetic model that describes the fermentation process in a medium containing a mixture of glucose, fructose and sucrose, such as date syrup.

In this study, the effect of scale up on the performance of *S. cerevisiae* will be investigated using three fermentors (0.5 L, 7.5 L and 80 L). Kinetic models, such as the modified Monod and Ghose–Tyagi, will be employed to study the effect on ethanol inhibition on the selective fermentation process. The modified Gompertz model will be expanded to enable the predictions of simultaneous fructose and ethanol production as well as fructose fraction in sugar.

2. Experimental

2.1. Yeast and propagation

The yeast of *S. cerevisiae* with the typical culture of ATCC 36858 was obtained from American Type Culture Collection (ATCC, Manassas, VA, USA). The microbe was then revived in accordance with the procedure of ATCC. It was further incubated in an agar slant. The yeast colony grown in the agar was then transferred to a sterilized liquid medium in a 500-mL flask and allowed to propagate for 36 h at 30°C and 120 rpm in a water bath shaker (Julabo SW23, Allentwon, USA). The agar and liquid medium contained 10-g dextrose, 3-g malt extract, 3-g yeast extract, 5-g peptone and de-ionized water (up to 1 L)

For yeast cultivation, 2 L of liquid medium containing 6-g malt extract, 6-g yeast extract, and 10-g peptone was prepared and poured into 7.5-L fermentor. The fermentor was then sterilized in an autoclave (Astell AMB230N, Sidcup, Kent, UK) at 121°C for 15 min. The cooled yeast broth in the fermentor was then aerated with air 1 vvm and operated at 30°C and 200 rpm. About 2-L water containing 20-g glucose was then fed-batch to the fermentor as the glucose concentration in the solution was kept at less than 0.05 g/L to avoid ethanol production. The final cultivated yeast concentration obtained through this process was about 1.9 g/L.

2.2. Raw materials

Sugars (fructose and glucose) were initially extracted from the dates using deionized water at 50°C for 2 h. The weight ratio of water to the dates was 2.5. To remove the fibers, the syrups were then centrifuged for 6 min at 6500 rpm. Before used in the fermentation process, the final syrup was further sterilized at 121°C for 15 min in an autoclave (Astell AMB230N, Kent, UK)

2.3. Fermentation process

The final syrup sterilized (85%) and the liquid propagation medium containing high yeast (15%) were aseptically mixed to gain a syrup concentration about 130 g/L. The fermentation processes were experimentally conducted out in 500-mL Erlenmeyer flask, 7.5-L fermentor with 2 impellers, 6 blades each and 80-L fermentor with a 4-blade impeller with effective working volumes of 0.1, 4 and 40 L, respectively. Table 1 presents the major features and dimensions of bioreactors for 7.5 and 80 L. The flask was placed in the Julabo water bath shaker. The experiments were conducted at 33°C and 120 rpm. Detailed description of experiments and cultivation of cell mass is given in previous publications [11,25,30]

Table 1
Major dimensions of the fermentors.

Fermentor volume (L)	7.5	80.0
Height (H), m	0.32	0.64
Inside diameter (D), m	0.18	0.42
Working volume, L	4	40
Inoculum volume, L	0.6	6
Impeller diameter, m	0.06	0.21
Shaft length, m	0.30	0.60
Rotation speed, rpm	120	120
Temperature, °C	33	33

2.4. Sample analysis

A portion of the sample withdrawn from the fermentor was centrifuged at 15000 rpm to remove the cell mass from the solution. The supernatant containing the sugars and ethanol was analyzed by using high performance liquid chromatography (HPLC-Agilent 1200 Infinitely series, DE, USA) equipped with an Aminex-® column and RID detector (150 × 7.8 mm, BIO-RAD®, California, USA). The column was kept at temperature of 40°C, and the mobile phase was 0.1-mM sulfuric acid. The cell mass concentration was determined from the other portion of the withdrawn sample by using NucleoCounter® YC-100TM system (NucleoCounter YC-100, Enfield, CT, USA). The dry weight method was used to calibrate the NucleoCounter® and to occasionally double check the amount of cell mass.

2.5. Parameters calculation

The following definitions have been used in this work
Fructose yield:

$$Y_F = \frac{F_0 - F_T}{F_0} \times 100\% \qquad \text{[Equation 1]}$$

Y_F is the fructose yield (%). F_0 is the fructose concentration before fermentation (g/L), and F_T is the fructose concentration at the end of fermentation (g/L).

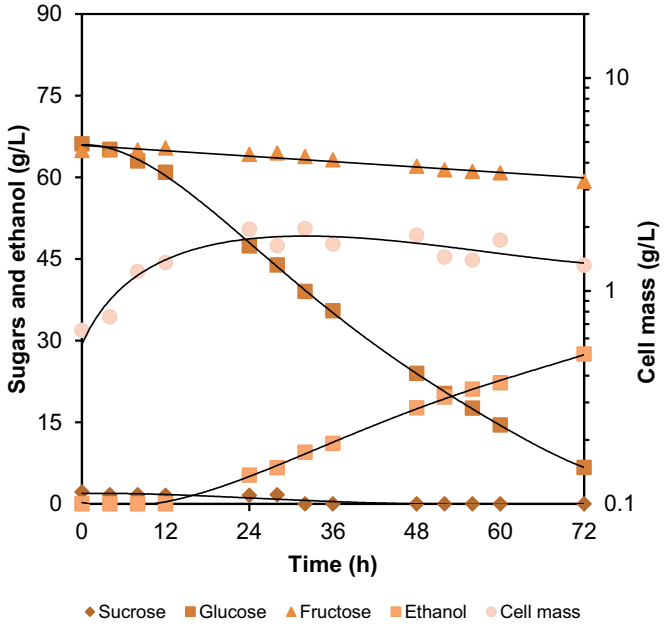

Fig. 1. The kinetic profile of sugars, ethanol and biomass for selective fermentation of date extract in 80-L fermentor.

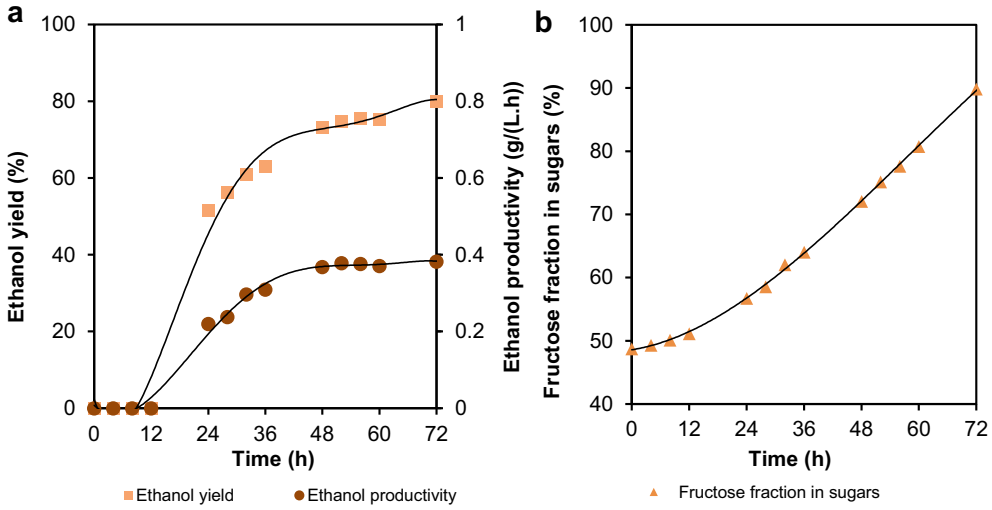

Fig. 2. The profiles of (a) ethanol yield and productivity; (b) fructose fraction in sugar in the 80-L fermentor.

Fructose fraction:

$$\eta = \frac{F_t}{S_t} \times 100\% \quad \text{[Equation 2]}$$

η is the fructose fraction in the syrup (%); F_t is the fructose concentration at a fermentation time (g/L), and S_t is the total concentration at the same fermentation time.

Ethanol yield:

$$Y_{P/S} = \frac{E_T - E_0}{(S_0 - S_T) \times 0.5114} \times 100\% \quad \text{[Equation 3]}$$

$Y_{P/S}$ is the ethanol yield based on its theoretical value in weight percent (%). E_0 and E_T are the ethanol concentration at the beginning of the fermentation and the end of the fermentation (g/L), respectively; while S_0 and S_T are the total concentration at the beginning of the fermentation and the end of the fermentation (g/L), respectively.

Ethanol productivity:

$$Q_P = \frac{E_T - E_0}{t_T - t_0} \quad \text{[Equation 4]}$$

Q_P is the volumetric ethanol productivity (g/(L·h)). E_0 and E_T are the ethanol concentration at the beginning and end of fermentation (g/L), respectively; while t_0 and t_T are the fermentation time at the beginning of the fermentation and the end of the fermentation (g/L), respectively.

3. Results and discussion

3.1. Selective fermentation of date syrup in the 80-L fermentor

Fig. 1 shows the profiles of the selective fermentation in the 80-L fermentor at 33°C by employing *S. cerevisiae* ATCC 36858. The profiles of the yield and productivity of ethanol and fructose fraction are given in Fig. 2a and Fig. 2b, respectively. The glucose has been selectively converted by the yeast to grow and to form ethanol. Very small fructose losses were observed during fermentation. Although fructose losses were observed in the range 36–76 h, the fructose loss rate was only less than one-eighth of the glucose loss rate in the range 0–72 h. As shown in Fig. 2a, the fructose fraction in sugar gradually increased and reached about 90% at 72 h (Table 2).

At the beginning stages of the fermentation, glucose was essentially used for growing. As shown in the cell mass profile, the phase of exponential growth took place within the first 24 h. During the 24 h, the cell mass weight increased from 0.6 to 2.0 g/L (Fig. 2); this led to the values of 0.69 h^{-1} and 0.064 g/g for the specific growth rate and the yield of cell mass, respectively. This growth inhibition was probably due to the produced ethanol. While the production of ethanol began after 12 h of the fermentation; the growth was inhibited at 24 h. It has been reported that ethanol concentrations >5% inhibit cell growth in glucose fermentation by yeast [31]. The inhibition by ethanol was studied in a medium containing 90 g glucose/L by *S. cerevisiae* ATCC 36859 [32]; the growth was inhibited at ethanol concentration about 3%. In a recent study [30], the growth of *S. cerevisiae* ATCC 36858 in glucose-fructose media with high concentration (250 g/L) was inhibited at ethanol concentration about 2%; whereas in this investigation, growth was inhibited at about 1% concentration. It is worthy to note that in the two latter investigations the substrate concentrations were high enough to prompt a possible combination of substrate and product inhibitions. The maximum ethanol yield (80%) and productivity (0.38 g/(L·h)) were obtained at 72 h as shown in Fig. 2b.

3.2. Comparison of fructose and ethanol produced in the three fermentors

Fig. 3a and Fig. 3b show the fructose yield and ethanol concentration, respectively for 0.5-L, 7.5-L and 80-L fermentors. For all fermentors, the initial increase in fructose concentration was due to sucrose hydrolysis. With scale up, the decrease in fructose yield was accompanied by an increase in ethanol production as shown in Table 2. The higher loss of fructose observed in the 80-L fermentor resulted in higher ethanol production. The higher consumption of sugars in the larger fermentor could be related to the better mixing [28,33]. Furthermore, the baffle types and mixing devices affect the contact of sugars with the yeast; thus, affecting their performance. It has been reported that systems without baffles in a 50-L fermentor resulted in less consumption of glucose compared to the shaker [28]. Also, the sugar percent was 85% in the shake flask compared to 99% in a 5-L fermentor with baffle system [33]. The latter finding [33] agrees with the results obtained in

Table 2
Results of selective fermentation in the three fermentors.

Parameter	0.5 L	7.5 L	80 L
Glucose consumption (%)	90	90	98
Fructose yield (%)	99	92	90
Fructose fraction in sugar (%)	91	90	94
Ethanol yield (%)	69	75	83
Ethanol productivity (g/(L·h))	0.26	0.32	0.37
Ethanol concentration (g/L)	21	27	31

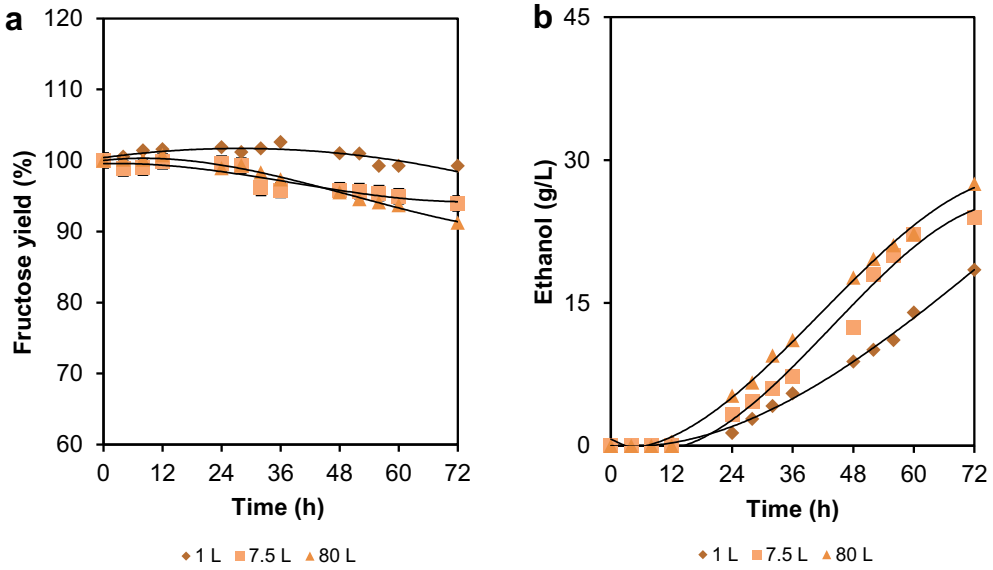

Fig. 3. The kinetic profile of (a) fructose yield; (b) ethanol production in the three fermentors.

this investigation (Table 2). From Table 2, it is obvious that better mixing decreased the yeast selectivity toward the sugars, as about 10% fructose losses were observed in the 80-L fermentor. However, this fructose loss is still in the range of the common performance of *S. cerevisiae* [26,34]. Though the H:D ratio for the 7.5-L and 80-L fermentors are almost equal, the difference in performance was probably due to the baffle system that affects the distribution of the substrate to the yeast.

It has also been noticed that higher ethanol yield was observed in the larger fermentor. This could also be attributed to better mixing that reduced localized ethanol inhibitions; a fact that was reaffirmed by the increase of ethanol productivity. This finding agrees with the reported results that ethanol inhibition suppresses microorganism growth, glucose consumption and ethanol productivity rates [35,36].

3.3. Kinetic models

Monod model could elucidate the behavior of cell growth, substrates and products concentration as well as their relationships. In this section, the profiles predicted by Monod kinetic model will be compared to experimental data of the 80-L fermentor. Inhibition by substrate is negligible here, since this type of inhibition will take place when the concentration of the substrate is higher than 150 g/L [37]. The equations below are proposed based on the Monod equation [29] and Ghose–Tyagi modification for inhibition by ethanol [38]:

$$\mu_1 = \mu_2 = \mu_{max}\left(\frac{S_G}{K_S + S_G}\right) \quad : \text{Monod} \qquad \text{[Equation 5]}$$

$$\mu_1 = \mu_{max}\left(\frac{S_G}{K_S + S_G}\right)\left(1 - \frac{P}{P_m}\right) \quad : \text{Gh—Ty} \qquad \text{[Equation 6]}$$

$$\mu_2 = \mu_{max}\left(\frac{S_G}{K_S + S_G}\right)\left(1 - \frac{P}{P_m'}\right) \quad : \text{Gh—Ty} \qquad \text{[Equation 7]}$$

$$\frac{dX}{dt} = \mu_1 . X \qquad \text{[Equation 8]}$$

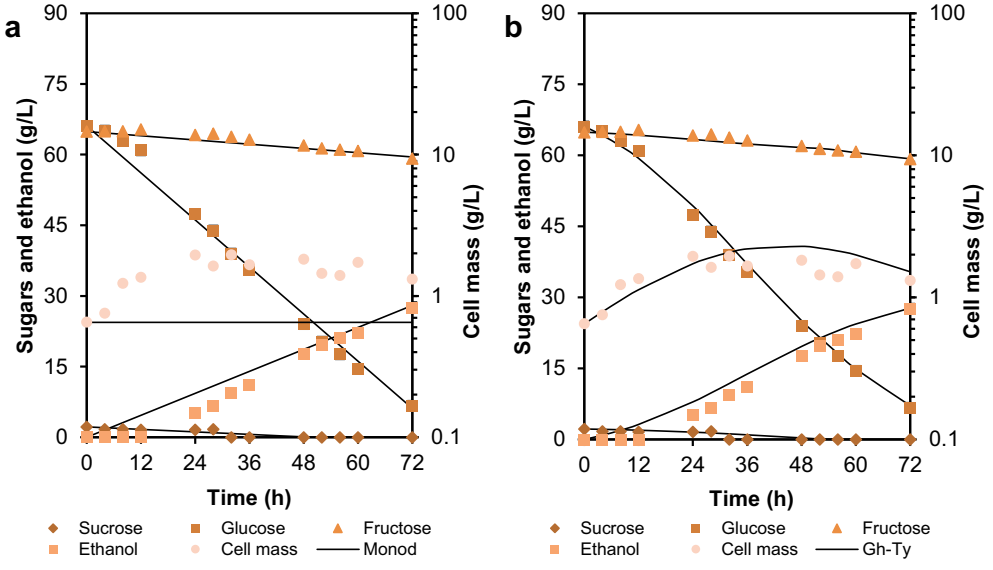

Fig. 4. Profiles of proposed kinetic model based on (a) Monod equation; (b) Ghose–Tyagi equation.

$$\frac{dS_{SC}}{dt} = -\alpha_S\left(\frac{S_{SC}}{K_{SC}+S_{SC}}\right)X \quad \text{[Equation 9]}$$

$$\frac{dS_G}{dt} = \alpha_S\left(\frac{S_{SC}}{K_{SC}+S_{SC}}\right)X\,Y_{G/SC} - \mu_2\,X\,\frac{1}{Y_{X/S}} \quad \text{[Equation 10]}$$

$$\frac{dS_F}{dt} = \alpha_S\left(\frac{S_{SC}}{K_{SC}+S_{SC}}\right)X\,Y_{F/SC} - \mu_2\,X\,\frac{R}{Y_{X/S}} \quad \text{[Equation 11]}$$

$$\frac{dP}{dt} = \mu_2\,X\,\frac{Y_{P/S}}{Y_{X/S}} \quad \text{[Equation 12]}$$

where S_G, S_F and S_{SC} are concentration of glucose, fructose and sucrose (g/L), respectively. K_S and K_{SC} are saturation constant for growth (g/L) and sucrose uptake (g/L), respectively. μ_{max} and α_S are specific cell mass growth rate (h^{-1}) and specific sucrose uptake rate (h^{-1}), respectively. $Y_{G/SC}$ and $Y_{F/SC}$ are the yield coefficients of glucose (g/g) and fructose (g/g) respectively which are equal, while $Y_{X/S}$ is the yield coefficient of cell mass (g/g). R is the ratio of glucose to fructose consumption rate. P is ethanol concentration during fermentation (g/L). $Y_{P/S}$ and $Y_{X/S}$ are the yield coefficient of ethanol (g/g) and cell mass (g/g), respectively. P_m (g/L) and P_m' (g/L) are the potential lowest ethanol concentrations at which cell growth is inhibited, and the yeast will no longer produces ethanol respectively.

The specific growth based on Monod equation is described by [Equation 5]. To account for ethanol inhibitions, Ghose and Tyagi [38] proposed [Equation 6 and Equation 7]. [Equation 8] presents the rate of cell mass production. [Equation 9] relates the sucrose uptake rate to the sucrose and cell mass concentration. The first term in [Equation 10] relates to the rate of sucrose uptake, while the second corresponds to cell mass production. In [Equation 11], the fructose rate is similar to that for glucose with an additional parameter (R). This proportionality constant (R) relates the rate of the fructose consumption to the rate of the glucose consumption. The ethanol production rate is given by [Equation 12].

The comparison between the Monod and Ghose–Tyagi kinetic model predictions with the experimental data are shown in Fig. 4a and Fig. 4b, respectively. A good overall fit was obtained with Monod model ($R^2 = 0.981$). The poor fit of the cell mass profile (Fig. 4a) could be related to the absence of growth inhibition by ethanol term in Monod equation. On the other hand, a better fit ($R^2 = 0.991$ (Table 3)) was obtained with Ghose–Tyagi model, especially the cell mass profile (Fig. 4b). This result reaffirms the importance of including growth inhibition caused by ethanol in model equations as discussed previously. The coefficient of ethanol yield, $Y_{P/S}$, (0.434) obtained here is quite close to 0.476, 0.47 and 0.466 that were reported by Bialas et al. [39], Ghose and Tyagi [38] and Koren and Duvnjak [32], respectively, although the coefficient of cell mass yield ($Y_{X/S}$) found here was lower. The lower value of P_m (18.0) compared to P_m' (53.6) indicates that the growth is powerfully inhibited by the ethanol; this phenomena has been observed in many microbial cases [35]. It has been reported that the decrease in ethanol tolerance of some *Saccharomyces* yeasts is enhanced by the slower rates of consumption of fructose compared to that of glucose [40]. Ethanol could damage the DNA of yeast cell mitochondria and subsequently inhibit its growth [41].

3.4. Product predictive models

This section presents models that concentrate on the kinetics and product formation. Such models are very valuable for further process developments and industrial application [42] of this group, the modified Gompertz model [Equation 13] will be used. This model was first developed for predicting the growth of microbes and was further used for the prediction of the ethanol production. It is initially used here to predict the production of the fructose. The Gompertz model is advantageous in predicting the lag time phase, the rate of the specific production and also the obtained maximum product [43,44]. The modified Gompertz equation here is further modified to fit fructose profile as follows:

Table 3
Predicted parameter for proposed models based on Monod and Ghose–Tyagi equation.

Parameter	Predicted value	
	Monod	Ghose–Tyagi
K_S (g/L)	0.0080	0.0051
α_S	0.0683	0.0240
K_{SC}	0.0017	0.0028
$Y_{X/S}$ (g/g)	0.0001	0.0703
$Y_{P/S}$ (g/g)	0.4645	0.4341
$Y_{G/SC}$ (g/g)	0.0278	2.2403
μ_{max} (h^{-1})	0.0001	0.0503
R	0.0904	0.1652
P_m (g/L)	–	18.002
P_m' (g/L)	–	53.621
R^2	0.981	0.991

$$\gamma_i = \gamma_{i,0} + \gamma_{i,m}\,\exp\left[-\exp\left[\frac{r_{i,m}\cdot\exp(1)}{\gamma_{i,m}}(t_L - t) + 1\right]\right] \quad \text{[Equation 13]}$$

where i indicates either fructose (Frcts) or ethanol (Eth). In the term of ethanol, the symbol of γ_{Eth} is used for the ethanol concentration (g/L); the symbol of $\gamma_{Eth,0}$ is the initial concentration of the ethanol (g/L) which is zero, $\gamma_{Eth,m}$ represents the potential maximum concentration of the ethanol (g/L); the symbol of $r_{Eth,m}$ is intended for the maximum rate of the ethanol production (g/(L·h)), and symbol of t_L represents the time at the exponential condition of the ethanol production (hour). In the term of fructose, the symbol of γ_{Frcts} is intended for the concentration of fructose (g/L); the symbol of $\gamma_{Frcts,0}$ represents the initial concentration of the fructose (g/L); the symbol $\gamma_{Frcts,m}$ is the potential drop of fructose (g/L); the symbol of $r_{Frcts,m}$ is intended for the maximum rate of the fructose loss (g/(L·h)), and t_L represents the time at the exponential drop of fructose (h).

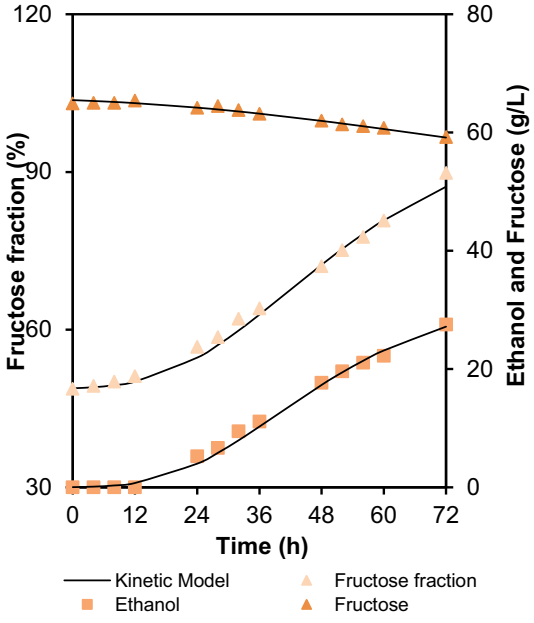

Fig. 5. Profile of individual kinetic model predictions against experimental data in the 80-L fermentor.

Table 4
Predicted parameters for individual kinetic models of fructose fraction, productions of ethanol and fructose in the 80-L fermentor.

Working volume, L	Parameters											
	Ethanol				Fructose				Fraction of fructose			
	$\gamma_{Eth,m}$ (g/L)	$r_{Eth,m}$ (g/(L·h))	t_L	R^2	$-\gamma_{Frcts,m}$ (g/L)	$-r_{Frcts,m}$ (g/(L·h))	t_L	R^2	$\eta_{Ffrac,m}$ (g/L)	$r_{Ffrac,m}$	t_L	R^2
0.1	28.7	0.40	26.5	0.994	1.496	0.045	21.3	0.852	99.0	0.83	18.6	0.982
4.0	31.0	0.55	21.2	0.992	13.34	0.081	17.4	0.944	99.0	0.66	20.9	0.981
40.0	33.2	0.60	18.9	0.995	18.45	0.121	15.5	0.989	99.0	0.80	18.4	0.990

Table 5
Predicted parameters for generalized model for the fructose fraction in syrup, productions of ethanol and fructose.

Parameter	Ethanol	Fructose	Fraction of fructose
γ_{i1} (g/L)	0.739	−2.865	99.0
γ_{i2} (g/L)	30.28	−8.448	–
r_{i1} (g·L/h)	0.034	−0.010	0.00119
r_{i2} (g/h)	0.485	−0.070	0.0485
r_{i3} (g/(L·h))	–	–	0.835
$\theta_{L,i1}$ (h/(L)^2)	−1.284	−0.972	−0.0165
$\theta_{L,i2}$ (h/L)	23.39	18.98	0.658
$\theta_{L,i3}$ (h)	–	–	18.53
R^2	0.989	0.919	0.983

The same model was expanded by our group [Equation 14] to facilitate the predictions of the fructose fraction.

$$\eta_{Ffrac} = \eta_{Ffrac,0} + \left(\eta_{Ffrac,m} - \eta_{Ffrac,0}\right) \exp\left[-\exp\left[\frac{r_{Ffrac,m}\cdot \exp(1)}{\left(\eta_{Ffrac,m} - \eta_{Ffrac,0}\right)}(t_L - t) + 1\right]\right]$$

[Equation 14]

where η_{Ffrac} represents the fructose fraction in syrup (%); the symbol of $\eta_{Ffrac,0}$ is intended for the initial fructose fraction in syrup (%); in this case the value is 47.45%, the symbol of $\eta_{Ffrac,m}$ represents the potential maximum concentration of the fructose fraction in syrup (%), the

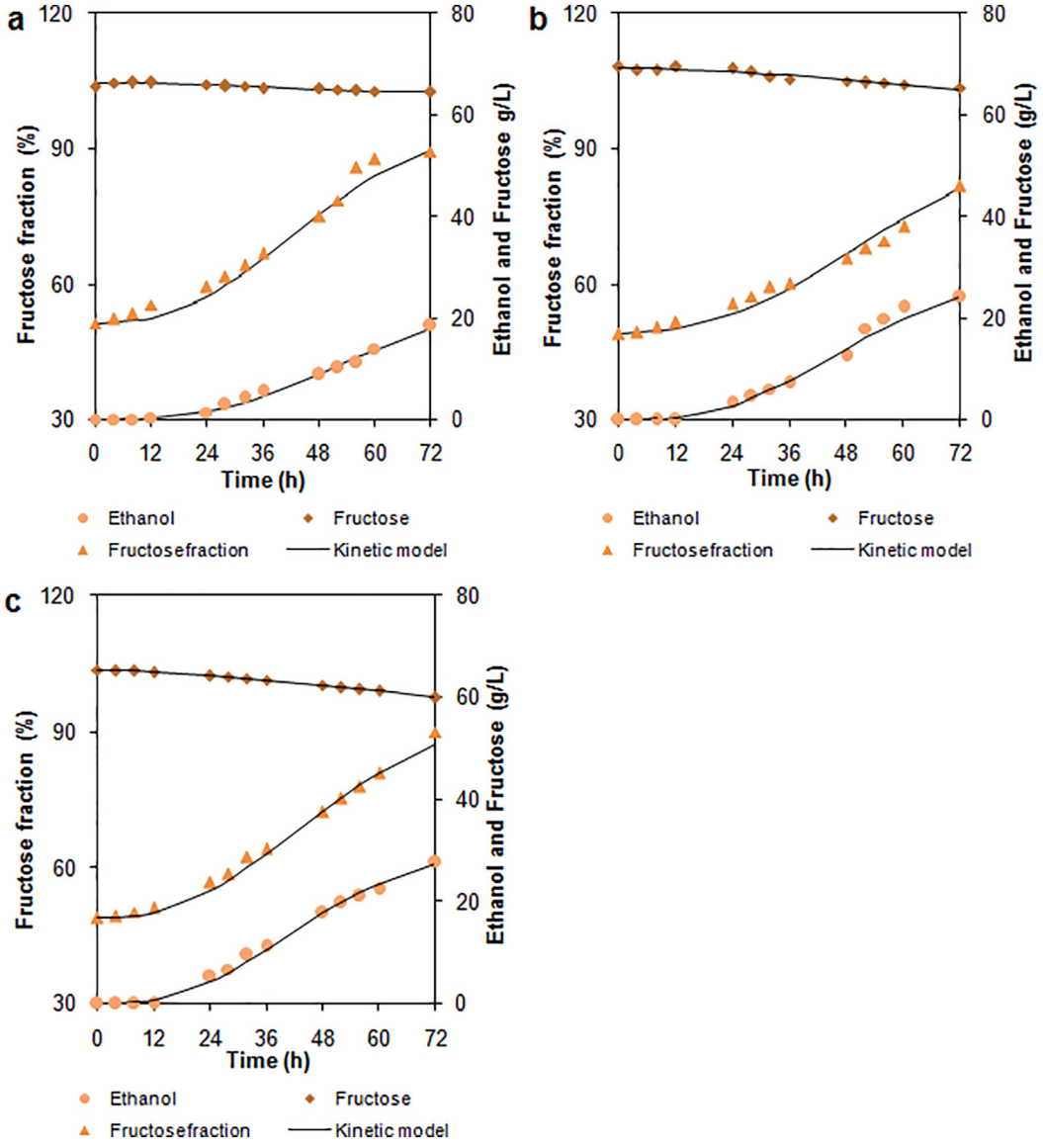

Fig. 6. Profiles of kinetic models predictions against experimental data for the fructose fraction, the ethanol and fructose productions for fermentation conducted in: (a) 0.5 L; (b) 7.5 L; (c) 80 L.

symbol of $r_{Ffrac,m}$ is intended for the maximum concentration of the fructose fraction in syrup (%), and the symbol of t_L represents the time at the exponential concentration of the fructose fraction (h).

Fig. 5 shows the excellent fitting between kinetic model predictions and the experimental data conducted in 80 L. The fitting is much better than that obtained using Monod or Ghose–Tyagi models; especially for ethanol production. As shown in Table 4, increasing the fermentor volume led to a higher maximum ethanol production rate ($r_{Eth,m}$), thereby giving the higher possible maximum concentration of the ethanol ($\gamma_{Eth,m}$). Higher maximum rate of fructose loss ($r_{Frcts,m}$) was also observed at higher volume; the negative sign in $r_{Frcts,m}$ designates the consumption of the fructose during the fermentation. In addition, our proposed expansion of the modified Gompertz equation for predicting fructose fraction in sugar well-fitted with the experimental data (Fig. 5). This expanded equation is helpful to predict the fermentation time desired to expect a fructose fraction in syrup.

In order to expand the predictability range of the model so that it could be used for further process development and industrial implementation, the data obtained in the three fermentors (0.5 L, 7.5 L and 80 L) was combined to produce a more generalized equation. The parameters of the model were expressed in terms of fermentors volume as given by [Equation 15, Equation 16, Equation 17, Equation 18, Equation 19, Equation 20] below

$$\gamma_{i,m} = \gamma_{i1}\ \ln(V) + \gamma_{i2} \quad \text{[Equation 15]}$$

$$r_{i,m} = r_{i1}\ \ln(V) + r_{i2} \quad \text{[Equation 16]}$$

$$t_{L,i} = \theta_{L,i1}\ \ln(V) + \theta_{L,i2} \quad \text{[Equation 17]}$$

$$\eta_{Ffrac,m} = \gamma_{i1} \quad \text{[Equation 18]}$$

$$r_{Ffrac,m} = r_{i1}V^2 + r_{i2}V + r_{i3} \quad \text{[Equation 19]}$$

$$t_{L,Ffrac} = \theta_{L,i1}V^2 + \theta_{L,i2}V + \theta_{L,i3} \quad \text{[Equation 20]}$$

where i denotes ethanol, fructose or fructose fraction; γ_{i1}, γ_{i2}, r_{i1}, r_{i2}, r_{i3}, $\theta_{L,i1}$, $\theta_{L,i2}$ and $\theta_{L,i3}$ are constants, and V is the working volume of the fermentors used, i.e., 0.1, 4 and 40 L. The values of the constants are presented in Table 5.

Fig. 6a, Fig. 6b and Fig. 6c present the model predictions against the experimental data for fructose fraction, ethanol and fructose production in the 0.5-L, 7.5-L and 40-L fermentors, respectively. Excellent fit for the three fermentors was obtained as evidenced by the values of R^2 given in Table 5.

4. Conclusions

Date fruits provide renewable and sustainable sources for the simultaneous production of fructose and ethanol by selective fermentation. *S. cerevisiae* ATCC 36858 was used in three fermentors (0.5 L, 7.5 L and 80 L). These scales were used to explore the commercial potential of this process. Higher consumptions of the glucose and fructose as well as the ethanol production were obtained in the larger fermentor. The ethanol concentrations were 21, 27 and 31 g/L, and the achieved fructose yields were 99, 92 and 90% in fermentors of 0.5 L, 7.5 L and 80 L, respectively. The proposed kinetic model combined with Monod and Ghose–Tyagi equation fitted the experimental data quite well. The fittings revealed the importance of including ethanol inhibition in the yeast growth data. The modified Gompertz model was expanded to include the effect of fermentor size on performance; better fits were obtained with such a model. This will be useful for utilization of the models in industrial application for commercial purpose.

Conflict of interest

The authors report no relationships that could be construed as a conflict of interest.

Acknowledgements

The authors extend their appreciation to King Saud University, Deanship of Scientific Research, College of Engineering Research Center for supporting this research.

References

[1] Lemos DA, Sonego JLS, Boschiero MV, et al. AC. Selection and application of nontoxic solvents in extractive ethanol fermentation. Biochem Eng J 2017;127:128–35. https://doi.org/10.1016/j.bej.2017.08.003.
[2] Achinas S, Euverink GJW. Consolidated briefing of biochemical ethanol production from lignocellulosic biomass. Electron J Biotechnol 2016;23:44–53. https://doi.org/10.1016/j.ejbt.2016.07.006.
[3] Lopes ML, SCDL Paulillo, Godoy A, et al. Ethanol production in Brazil: a bridge between science and industry. Braz J Microbiol 2016;47(sup 1):64–76. https://doi.org/10.1016/j.bjm.2016.10.003.
[4] Rass-Hansen J, Falsig H, Jørgensen B, et al. Bioethanol: fuel or feedstock? J Chem Technol Biotechnol 2007;82:329–33. https://doi.org/10.1002/jctb.1665.
[5] Qiu C, Colson G, Wetzstein M. An ethanol blend wall shift is prone to increase petroleum gasoline demand. Energy Econ 2014;44:160–5. https://doi.org/10.1016/j.eneco.2014.04.005.
[6] Sun Y, Cheng J. Hydrolysis of lignocellulosic materials for ethanol production: a review. Bioresour Technol 2002;83(1):1–11. https://doi.org/10.1016/S0960-8524(01)00212-7.
[7] Zakaria Z, Kamarudin SK, Timmiati SN. Membranes for direct ethanol fuel cells: an overview. Appl Energy 2016;163:334–42. https://doi.org/10.1016/j.apenergy.2015.10.124.
[8] Ruiz MI, Sanchez CI, Torrres RG, et al. Enzymatic hydrolysis of cassava starch for production of bioethanol with a Colombian wild yeast strain. J Braz Chem Soc 2011;22: 2337–43. https://doi.org/10.1590/S0103-50532011001200014.
[9] Yu H, Guo Y, Wu D, et al. Immobilization of glucose isomerase onto GAMM support for isomerization of glucose to fructose. J Mol Catal B Enzym 2011;72(1–2):73–6. https://doi.org/10.1016/j.molcatb.2011.05.006.
[10] Nabors L. Alternative sweeteners. 3rd ed. New York, NY: Marcel Dekker; 2001 [374 pp.].
[11] Putra MD, Abasaeed AE, Atiyeh HK, et al. Kinetic modeling and enhanced production of fructose and ethanol from date fruit extract. Chem Eng Commun 2015;202(12): 1618–27. https://doi.org/10.1080/00986445.2014.968711.
[12] Jain SM. *In vitro* mutagenesis for improving date palm (*Phoenix dactylifera* L.). Emir J Food Agric 2012;24:400–7.
[13] Moshaf S, Hamidi-Esfahani Z, Azizi MH. Optimization of conditions for xanthan gum production from waste date in submerged fermentation. World Acad Sci Eng Technol 2011;57:521–4.
[14] Zhang Y, Hidajat K, Ray AK. Optimal design and operation of SMB bioreactor: production of high fructose syrup by isomerization of glucose. Biochem Eng J 2004; 21:111–21. https://doi.org/10.1016/j.bej.2004.05.007.
[15] Gaily MH, Elhassan BM, Abasaeed AE, et al. Isomerization and kinetics of glucose into fructose. Int J Eng Technol 2010;3:1–10.
[16] Abasaeed AE, Lee YY. Inulin hydrolysis to fructose by a novel catalyst. Chem Eng Technol 1995;18:440–4. https://doi.org/10.1002/ceat.270180612.
[17] Di Luccio M, Borges CP, Alves TLM. Economic analysis of ethanol and fructose production by selective fermentation coupled to pervaporation: effect of membrane costs on process economics. Desalination 2002;147:161–6. https://doi.org/10.1016/S0011-9164(02)00526-X.
[18] AlNashef IM, Gaily MH, Al-Zahrani SM, Abasaeed AE. Method for separating fructose and glucose, U. Patent Ed., USA (2011).
[19] Lima DM, Fernandes P, Nascimento DS, et al. Fructose syrup: a biotechnology asset. Food Technol Biotechnol 2011;49:424–34.
[20] Moulik S, Vadthya P, Kalipatnapu YR, et al. Production of fructose sugar from aqueous solutions: Nanofiltration performance and hydrodynamic analysis. J Clean Prod 2015;92:44–53. https://doi.org/10.1016/j.jclepro.2014.12.092.
[21] Tajima T, Tomita K, Miyahara H, et al. Efficient conversion of mannitol derived from brown seaweed to fructose for fermentation with a thraustochytrid. J Biosci Bioeng 2017;125(2):180–4. https://doi.org/10.1016/j.jbiosc.2017.09.002.
[22] Haque MA, Yang X, Ong KL, et al. Bioconversion of beverage waste to high fructose syrup as a value-added product. Food Bioprod Process 2017;105:179–87. https://doi.org/10.1016/j.fbp.2017.07.007.
[23] Zhan W, Jin L, Jiao J, et al. Expression and purification of plant fructan exohydrolases and their potential applications in fructose production. Int J Biol Macromol 2018; 108:9–17. https://doi.org/10.1016/j.ijbiomac.2017.11.110.
[24] Singh RS, Chauhan K, Kennedy JF. A panorama of bacterial inulinases: production, purification, characterization and industrial applications. Int J Biol Macromol 2017; 96:312–22. https://doi.org/10.1016/j.ijbiomac.2016.12.004.
[25] Putra MD, Abasaeed AE. Prospective production of fructose and ethanol for food and fuel markets by selective fermentations of date syrups. Appl Eng Agric 2015;31(3): 497–504. http://dx.doi.org/10.13031/aea.31.10759.
[26] Carvalho R, Gomes L, Gonzaga do P, Filho L, et al. Obtaining and selection of hexokinases-less strains of *Saccharomyces cerevisiae* for production of ethanol and fructose from sucrose. Appl Microbiol Biotechnol 2008;77:1131–7. https://doi.org/10.1007/s00253-007-1251-y.

[27] Atiyeh H, Duvnjak Z. Production of fructose and ethanol from cane molasses using *Saccharomyces cerevisiae* ATCC 36858. Acta Biotechnol 2003;23(1):37–48. https://doi.org/10.1002/abio.200390005.
[28] Nuanpeng S, Laopaiboon L, Srinophakun P, et al. Ethanol production from sweet sorghum juice under very high gravity conditions: batch, repeated-batch and scale up fermentation. Electron J Biotechnol 2011;14(1):1–12. https://doi.org/10.2225/vol14-issue1-fulltext-2.
[29] Monod J. The growth of bacterial cultures. Annu Rev Microbiol 1949;3:371–94. https://doi.org/10.1146/annurev.mi.03.100149.002103.
[30] Putra MD, Abasaeed AE, Al-Zahrani SM, et al. Production of fructose from highly concentrated date extracts using *Saccharomyces cerevisiae*. Biotechnol Lett 2014;36(3):531–6. https://doi.org/10.1007/s10529-013-1388-y.
[31] Shuler ML, Kargi F. Bioprocess engineering basic concepts. 2nd ed. Upper Saddle River, New Jersey, USA: Prentice-Hall, Inc.; 2002 [517 pp.].
[32] Koren DW, Duvnjak Z. Kinetics of the selective fermentation of glucose from glucose/fructose mixtures using *Saccharomyces cerevisiae* ATCC 36859. Acta Biotechnol 1993;13:311–22. https://doi.org/10.1002/abio.370130402.
[33] Ogbonna JC, Mashima H, Tanaka H. Scale up of fuel ethanol production from sugar beet juice using loofa sponge immobilized bioreactor. Bioresour Technol 2001;76(1):1–8. https://doi.org/10.1016/S0960-8524(00)00084-5.
[34] Koren DW, Duvnjak Z. Continuous production of fructose syrup and ethanol from hydrolysed Jerusalem artichoke juice. J Ind Microbiol 1991;7(2):131–5. https://doi.org/10.1007/BF01576075.
[35] Van Uden N. Ethanol toxicity and ethanol tolerance in yeasts. Annu Rep Ferment Process 1985;8:11–58. https://doi.org/10.1016/B978-0-12-040308-0.50006-9.
[36] Phisalaphong M, Srirattana N, Tanthapanichakoon W. Mathematical modeling to investigate temperature effect on kinetic parameters of ethanol fermentation. Biochem Eng J 2006;28(1):36–43. https://doi.org/10.1016/j.bej.2005.08.039.
[37] Thatipamala R, Rohani S, Hill GA. Effects of high product and substrate inhibitions on the kinetics and biomass and product yields during ethanol batch fermentation. Biotechnol Bioeng 1992;40:289–97. https://doi.org/10.1002/bit.260400213.
[38] Ghose TK, Tyagi RD. Rapid ethanol fermentation of cellulose hydrolysate. II. Product and substrate inhibition and optimization of fermentor design. Biotechnol Bioeng 1979;21:1401–20. https://doi.org/10.1002/bit.260210808.
[39] Bialas W, Czerniak A, Szymanowska-Powałowska D. Kinetic modeling of simultaneous saccharification and fermentation of corn starch for ethanol production. Acta Biochim Pol 2014;61(1):153–62.
[40] De la Torre-González FJ, Narváez-Zapata JA, López-y-López VE, et al. Ethanol tolerance is decreased by fructose in *Saccharomyces* and non-*Saccharomyces* yeasts. LWT Food Sci Technol 2016;67:1–7. https://doi.org/10.1016/j.lwt.2015.11.024.
[41] You KM, Rosenfield C-L, Knipple DC. Ethanol tolerance in the yeast *Saccharomyces cerevisiae* is dependent on cellular oleic acid content. Appl Environ Microbiol 2003;69(3):1499–503. https://doi.org/10.1128/aem.69.3.1499-1503.2003.
[42] Gorsek A, Zajsek K. Influence of temperature variations on ethanol production by Kefir grains - mathematical model development. Chem Eng Trans 2010;20:181–6. https://doi.org/10.3303/CET1020031.
[43] Zajsek K, Gorsek A. Modelling of batch kefir fermentation kinetics for ethanol production by mixed natural microflora. Food Bioprod Process 2010;88(1):55–60. https://doi.org/10.1016/j.fbp.2009.09.002.
[44] Mu Y, Wang G, Yu HQ. Kinetic modeling of batch hydrogen production process by mixed anaerobic cultures. Bioresour Technol 2006;97(11):1302–7. https://doi.org/10.1016/j.biortech.2005.05.014.